# Enhanced Catalytic Transfer Hydrogenation of Ethyl Levulinate to γ-Valerolactone over a Robust Cu−Ni Bimetallic Catalyst

Bo Cai,[‡] Xin-Cheng Zhou,[‡] Ying-Chun Miao, Jin-Yue Luo, Hui Pan,*[iD] and Yao-Bing Huang*[iD]

College of Chemical Engineering, Nanjing Forestry University, No. 159 Longpan Road, 210037 Nanjing, China

S Supporting Information

ABSTRACT: An efficient and robust bimetallic catalyst has been developed for the transfer hydrogenation of biomass derived ethyl levulinate to γ-valerolactone with 2-butanol as the hydrogen donor. Several bimetallic catalysts were prepared and characterized by Brunauer−Emmett−Teller, transmission electron microscopy, X-ray power diffraction and X-ray photoelectron spectrometry. They exhibited different catalytic activities in the catalytic transfer hydrogenation (CTH) reaction. Results showed that 10Cu-5Ni/Al₂O₃ had the highest activity, providing a 97% yield of GVL product in 12 h at 150 °C. The reaction temperature, reaction time and catalyst loading were also investigated and found to affect the product yield. The catalyst was also successfully applied to the CTH of various levulinate esters with different secondary alcohols. Comparing experiments between Cu−Ni and Cu catalysts and the poisoning experiments revealed that the introduction of Ni to Cu remarkably enhanced the catalyst's activity and stability, showing an outstanding recycling ability in the 10 runs recycling experiments without notable loss in the activity.

KEYWORDS: Ethyl levulinate, γ-Valerolactone, Transfer hydrogenation, Bimetallic catalyst, Stability
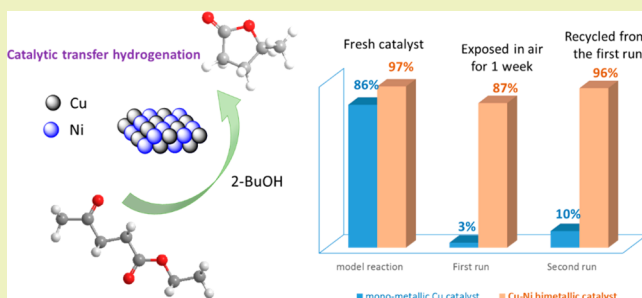
■ INTRODUCTION

The utilization of renewable biomass to produce energy has been considered as a promising solution to the energy crisis and the pollution caused by fast and huge consumption of fossil resources.[1,2] The biorefinery industry can produce carbon-containing molecules for drugs or liquid fuels, which are beyond the scope of other renewable energies (e.g., solar, wind).[3] Among various biomass feedstocks, lignocellulose is getting more attention due to its abundance and low cost. It can be easily converted to a variety of molecules including alkanes/alkenes,[4−6] polyols,[7−11] acids,[12−15] esters[16−18] and aldehydes.[19,20] For example, hydrolysis/alcoholysis of cellulose in aqueous/alcoholic solutions provide the important platform chemicals levulinic acid (LA)/levulinate esters.[16−18] Through the downstream processing, they can be easily converted to several useful products such as γ-valerolactone (GVL),[21,22] valerate esters[23,24] and 1,4-pentanediol.[25,26] Of all these compounds, GVL is the most widely studied molecule with numerous applications such as a fuel additive, solvent, precursor for the production of other chemicals.[21,22]

To date, many processes have been developed for the production of GVL from LA through hydrogenation reaction.[27] These reactions were mainly conducted in the presence of hydrogen with various metal catalysts such as Ir,[28] Rh,[28] Pd,[29,30] Ru,[31−33] Pt,[34] Co,[35] Cu[36] and Ni.[37−40] In the past few years, formic acid (FA), an *in situ* hydrogen source, was also applied for the conversion of LA to GVL instead of an external H₂ gas. It was demonstrated as an effective and economical method when the upstream carbohydrate hydrolysate (LA and FA

aqueous solution) was used as the raw material.[41] Apart from LA, levulinate esters were also an appealing substrate for preparing GVL. They could be produced from cellulose in alcoholic solutions with high yield under mild conditions. Meanwhile, they are much easier and more energy-efficient to be separated from the alcoholic mixture than the separation of LA from water.[42,43] Therefore, it is attractive to develop more efficient systems for the catalytic hydrogenation of levulinate esters to GVL.

At the same time, the catalytic transfer hydrogenation (CTH) reaction has emerged as an alternative hydrogenating method to the conventional H₂ method for the reduction of carbonyl compounds,[44,45] which is the key step to convert LA or levulinate esters to GVL. For example, Dumesic et al.[46] reported the CTH of ethyl levulinate (EL) to GVL over ZrO₂ catalyst in the presence of isopropyl alcohol, H-donor solvent, at 150 °C. Lin et al.[47] found that zirconia based hydroxide ZrO(OH)₂ could effectively catalyze the CTH of EL to GVL in a supercritical ethanol solution. Song and Han et al.[48] used Zr-HBA as the CTH reaction catalyst and achieved 94.4% yield of GVL in isopropyl alcohol. Kuwahara et al.[49] demonstrated that ruthenium hydroxides supported on basic oxides could exhibit high catalytic activity in the CTH of EL to GVL. Our group has also reported the CTH of EL over Raney Ni catalyst with an almost quantitative yield at room temperature.[50] Several other

new systems were also reported as effective for the CTH conversion.[51−55] Nevertheless, there still exist some limitations of the above systems such as harsh reaction conditions, low catalyst stability and long reaction time, etc. Therefore, further improvement of the reaction efficiency of the CTH of levulinate esters to GVL with more robust catalyst is highly desired.

Previous research demonstrated that copper catalysts exhibited excellent catalytic activities in the CTH reactions for the production of various organic chemicals.[56] However, the low stability and easily oxidized nature of these catalysts severely restrict their applications in other areas. Therefore, a second metal was introduced to the copper catalyst to form a bimetallic catalyst in this study, which can not only stabilize the copper metal particle sites but also enhance the activity of the catalyst.[57,58] Herein, we reported a bimetallic Cu−Ni catalyst for the CTH of levulinate esters to GVL in the presence of 2-buthanol as the H-donor (Scheme 1). Several other bimetallic

Scheme 1. Routes for the Production of GVL from Levulinic Acid/Esters
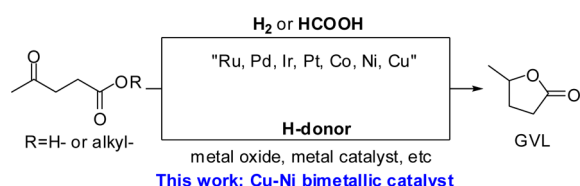
catalysts were also prepared, characterized and tested for the CTH reaction. The influences of the metal ratio, reaction conditions, as well as the stability and recyclability of the catalysts were investigated.

■ EXPERIMENTAL SECTION

Materials. Levulinate esters and γ-valerolactone were purchased from TCI Chemical Reagent Company (Shanghai, China). $Ni(NO_3)_2$·$6H_2O$, $Cu(NO_3)_2$·$6H_2O$ and solvents were purchased from Sinopharm Chemical Reagent Company (Shanghai, China). The metal oxide supports were purchased from Saint-Gobain NorPro Company (America). The other chemicals were purchased from local companies and used without further purification.

Preparation of the Catalysts. The catalysts were prepared by incipient impregnation method. In a typical procedure for preparing the $10\%Cu-5\%Ni/Al_2O_3$, 1.7 g of Al_2O_3 was first impregnated with a aqueous solution containing 0.753 g of $Cu(NO_3)_2$·$3H_2O$ and 0.495 g of $Ni(NO_3)_2$·$6H_2O$. Then the mixture was vigorously stirred for 12 h and dried at 110 °C for another 12 h. The resulted powder was grinded and calcined at 500 °C for 4 h. The catalyst was then reduced in a flow of 5% H_2/N_2 from room temperature to 500 °C at 10 °C/min, then kept at 500 °C for another 2 h. After cooling to room temperature, the catalyst was collected and weighed. This catalyst was denoted as $10\%Cu-5\%Ni/Al_2O_3$ ($10Cu-5Ni/Al_2O_3$). Other catalysts were prepared with a similar procedure as that for $10Cu-5Ni/Al_2O_3$.

Catalytic Reactions. Transfer hydrogenation of EL was carried out in a thick-wall pressured tube. For the model reaction with $10Cu-5Ni/Al_2O_3$: EL 1.0 mmol, catalyst $10Cu-5Ni/Al_2O_3$ 100 mg and solvent 2-butanol 3 mL were charged into the reaction tube with a magnetic stirrer. The tube was then purged with nitrogen to remove air. The reaction was allowed to react in a 150 °C oil bath for 12 h at a stirring speed of 600 rpm. Upon the end of the reaction, the tube was removed from oil bath and cooled down to room temperature, and the reaction mixture was sampled and subjected to product analysis.

To recycle the catalyst, the catalyst was centrifuged after the reaction and washed with 2-BuOH for 3 times. All the liquid was

collected, combined and subjected to GC analysis. The solid catalyst was directly added to the reaction tube for the next run.

Characterization Methods. The Brunauer−Emmett−Teller (BET) surface area, pore size and pore volume of the catalyst were measured by an Automatic Surface Area and Pore Analyzer (Tristar II 3020 M, Micromeritics). X-ray power diffraction (XRD) of the catalysts were recorded on the Rigaku D MAX III VC diffraction system. Transmission electron microscopy (TEM) were acquired on a JEOL-2010 electron microscope. X-ray photoelectron spectra were recorded on the Scientific Escalab 250-X-ray photoelectron spectrometry (XPS) instrument.

The reaction mixture was analyzed with gas chromatography−mass spectroscopy (GC−MS, Agilent 7890A, Agilent 5975C MSD) and GC (Agilent 7890A) with a DB-5 capillary column (30 m × 0.25 mm × 0.25 μm, Agilent). The temperature of column increased from 160 to 250 °C at a 15 °C/min rate. Naphthalene was used as the internal standard.

■ RESULTS AND DISCUSSION

Characterization of Catalysts. Figure 1 shows the XRD patterns of the Cu−Ni catalysts and the support Al_2O_3. Al_2O_3
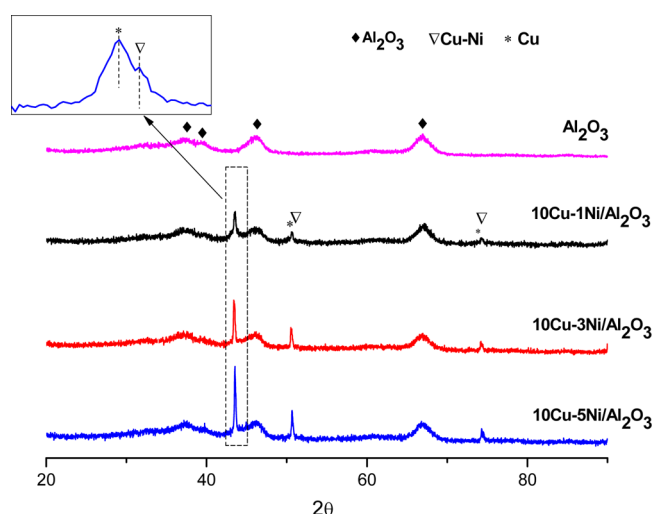
Figure 1. XRD analysis of the catalysts.

showed four typical reflection peaks at $2\theta = 37.4°$, 39.5°, 46.1° and 66.7°. These peaks can also be easily found in the as-prepared catalysts, indicating a well-dispersed alumina phase in these catalysts during the preparation process. Three new diffraction peaks were observed in the $10Cu-1Ni/Al_2O_3$ catalyst, which can be divided into two groups (partially overlapped, see amplification picture). One group was assigned to the metallic Cu phase (located at 43.3°, 50.4° and 74.1°), whereas the other was assigned to Cu−Ni alloy species (shoulder peaks located at 43.4°, 50.6° and 74.2°). These results were consistent with the results from the previously reported work.[59,60] No obvious diffraction peaks of metal oxides species (e.g., Cu_xO_y or Ni_xO_y) were observed in the XRD patterns, possibly attributed to their amorphous state or smaller size (<4 nm) that cannot be identified by XRD analysis. As the weight ratio of Ni increased in the catalysts, the diffraction peaks of Cu and Cu−Ni alloys became stronger. This change suggested that the increase in the Ni loading may result in more bimetallic Cu−Ni alloy species.

To explore further the chemical state of the metal sites, XPS analysis of the representative catalyst $10Cu-5Ni/Al_2O_3$ was carried out, and the results are present in Figure 2. For Cu
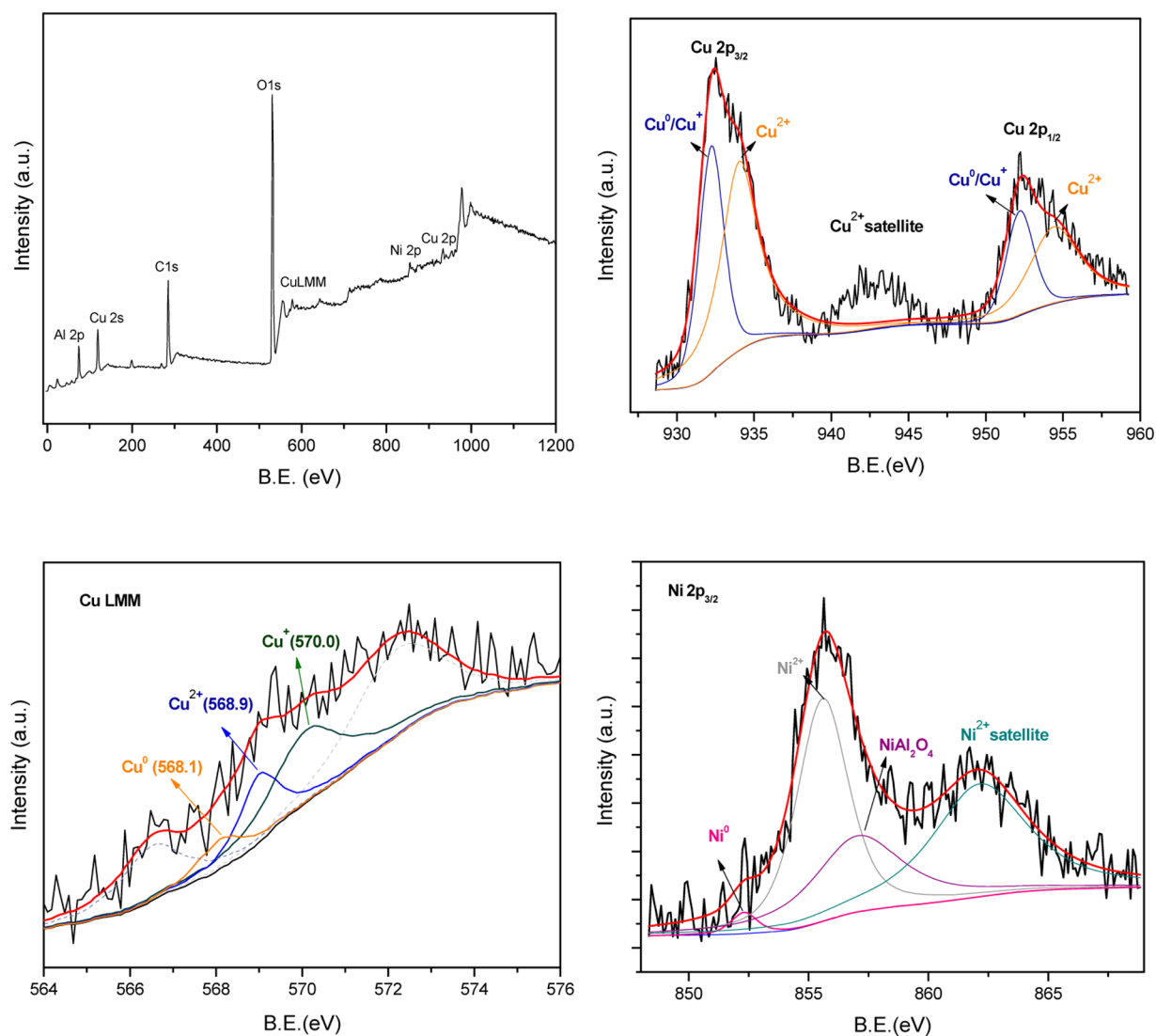
Figure 2. XPS analysis of the 10Cu-5Ni/Al$_2$O$_3$ catalyst: survey, Cu 2p, Cu LMM and Ni 2p.
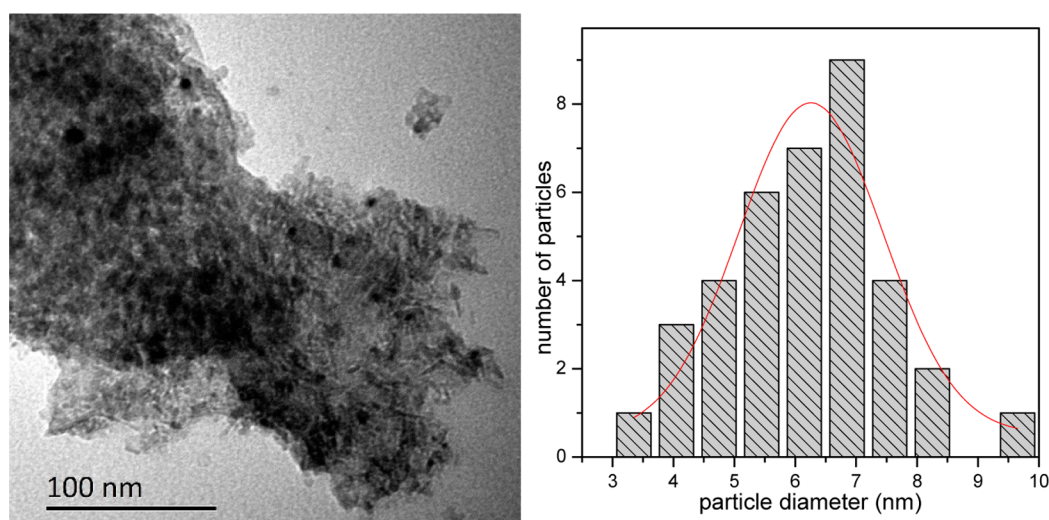

Figure 3. TEM analysis of the fresh 10Cu-5Ni/Al$_2$O$_3$ catalyst.
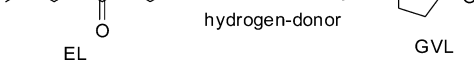
2p$_{3/2}$, the main peak at 932.3 eV corresponded to the Cu^0/Cu$^+$ species in the catalyst. Another peak at 934.2 eV, together with its satellite peak around 944 eV, was assigned to the CuO

species. Because the binding energies of Cu^0 and Cu$^+$ in Cu 2p$_{3/2}$ were very close, the Cu LMM Auger spectra were also recorded to distinguish these two species. The broad peak was

Table 1. Textural Properties of the Catalysts

entry	catalyst	S_{BET} (m²/g)[a]	V_p (cm³/g)[b]	D_p (nm)[c]
1	Al₂O₃	222.4	0.72	12.9
2	10Cu-1Ni/Al₂O₃	166.9	0.53	12.8
3	10Cu-3Ni/Al₂O₃	214.5	0.64	12.0
4	10Cu-5Ni/Al₂O₃	191.3	0.53	10.9
5	10Cu-5Ni/Al₂O₃(used)	143.5	0.36	10.1

[a]BET surface area. [b]Total pore volume. [c]Average pore size.

Table 2. Screening of the Catalysts for Transfer Hydrogenation of EL[a]

entry	catalyst	conv. (%)	GVL (%)[b]
1	10Cu-1Ni/Al₂O₃	98	90
2	10Cu-3Ni/Al₂O₃	98	92
3	10Cu-5Ni/Al₂O₃	100	97
4	15Cu-5Ni/Al₂O₃	90	84
5	10Cu-5Ni/TiO₂	6	2
6	10Cu-5Ni/SiO₂	0	0
7	10Cu-5Ni/SiO₂-Al₂O₃	93	91
8	10Cu-5Ni/ZrO₂	95	92
9	10Cu/Al₂O₃	92	86
10	5Ni/Al₂O₃	30	26
11	10Cu/Al₂O₃+5Ni/Al₂O₃	80	70
12[c]	10Cu-5Ni/Al₂O₃	92	87
13[d]	10Cu-5Ni/Al₂O₃	91	86
14	Al₂O₃	23	18

[a]Conditions: EL 1.0 mmol, catalyst 100 mg, 2-BuOH 3 mL, 150 °C, 12 h. [b]GC yield. [c]5 wt % H₂O was added. [d]conducted in the air.

Table 3. Influence of the Catalyst Loading on the CTH of EL[a]

entry	catalyst loading/mg (wt %)	conv. (%)	GVL (%)[b]
1	60 (6.25)	74	71
2	80 (8.33)	94	89
3	100 (10.42)	100	97
4	120 (12.50)	100	95
5[c]	60 (6.25)	100	96

[a]Conditions: EL 1.0 mmol, 10Cu-5Ni/Al₂O₃, 2-BuOH 3 mL, 150 °C, 12 h. [b]GC yield. [c]24 h. The data in parentheses was the total weight ratio of metals to EL.

Table 4. CTH of Different Levulinate Esters in Different H-Donor Solvent[a]

entry	substrate	alcohol	conv. (%)	GVL (%)[b]
1	EL	MeOH	7	5
2	EL	EtOH	9	8
3[c]	EL	2-PrOH	79 (92)	75(87)
4	EL	3-pentanol	100	97
5	EL	CyOH	89	81
6	ML	2-BuOH	100	94
7	BL	2-BuOH	100	95
8	LA	2-BuOH	10	6

[a]Conditions: levulinate ester 1.0 mmol, catalyst 100 mg, solvent 3 mL, 150 °C, 12 h. [b]GC yield. [c]reaction time was 24h (in the parentheses).

deconvoluted into five peaks, among which the peaks at 568.1 and 570.0 eV were assigned to the Cu⁰ and Cu⁺ species, respectively, whereas the peak at 568.9 eV was the Cu²⁺ species.[59] This result clearly highlighted the presence of three oxidation states of the Cu species. The determination of their concentrations by the deconvolution of the Auger peak was about 1:2.2:4.3 for Cu⁰, Cu²⁺ and Cu⁺. For Ni species, only a small peak of Ni⁰ (located at 852.3 eV) was observed in the Ni 2p₃/₂ XPS spectrum, implied that most of the Ni species

remained in the oxidative state in the as-prepared catalyst and. The dominate peak at 855.6 eV was assigned to the NiO crystallite species, which was further confirmed by its satellite peak at 862.5 eV. Another smaller peak located at 857.2 eV was assigned to the NiAl₂O₄ crystallite species,[61] which was reluctant to be reduced under the reduction condition. Combined with the earlier XRD analysis, it could be seen that both metallic and oxidized Cu and Ni crystallite species were present in the as-prepared 10Cu-5Ni/Al₂O₃ catalyst.

A typical TEM spectrum of the as-prepared catalyst 10Cu-5Ni/Al₂O₃ and the corresponding particle size distribution curve are present in Figure 3. The reduced catalyst showed a good dispersion of the metal sites on the Al₂O₃ supports, with an average particle size of 6−7 nm. This may be attributed to the interaction between the two metal sites, which helped to stabilize and disperse the metals into small particles during the
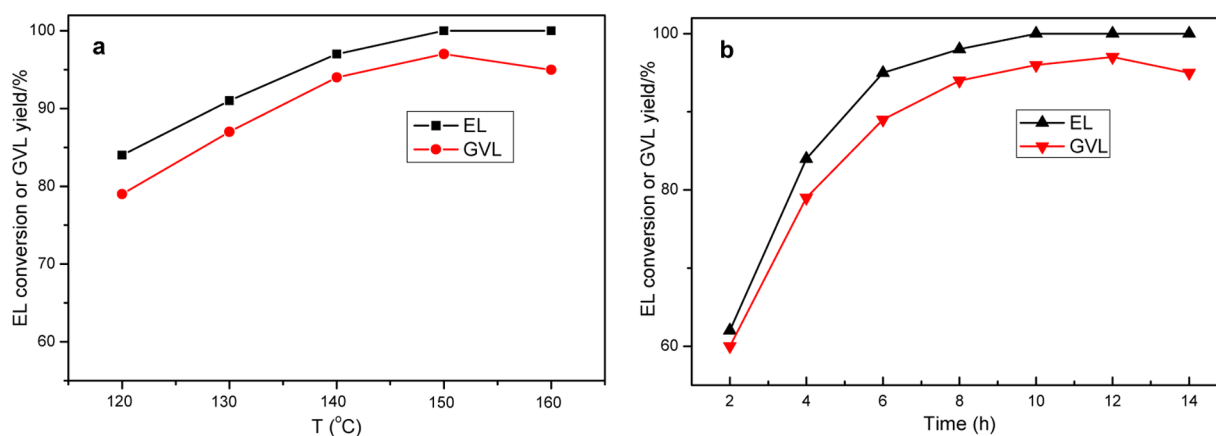

Figure 4. Influences of (a) reaction temperature and (b) reaction time on the reaction conversion and yield. Condition: EL 1.0 mmol, catalyst 100 mg, 2-BuOH 3 mL. (a) 12 h; (b) 150 °C.
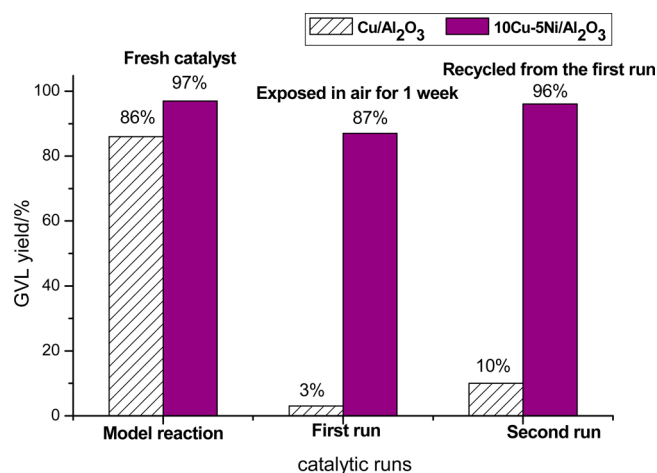
Figure 5. Investigation of the stability of catalyst. Conditions: EL 1.0 mmol, catalyst 100 mg, 2-BuOH 3 mL, 150 °C, 12 h.
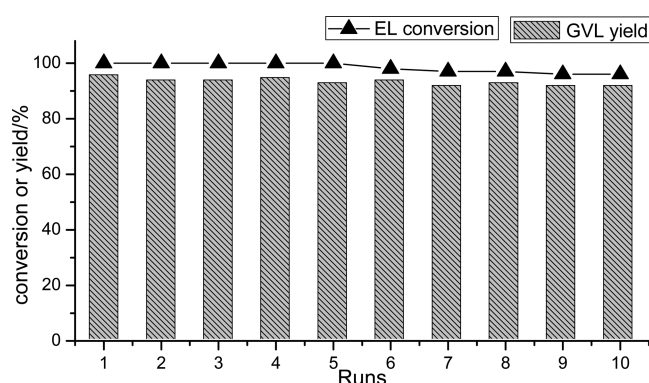

Figure 6. Recycling test of the catalyst. Conditions: EL 1.0 mmol, catalyst 100 mg, 2-BuOH 3 mL, 150 °C, 12 h.
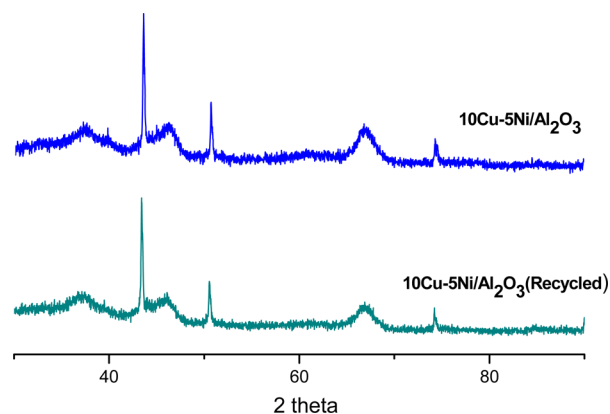

Figure 7. XRD analysis of the spent 10Cu-5Ni/Al$_2$O$_3$ catalyst.

reduction process. It would also help to enhance the reactivity of the resulting catalysts. For the monometallic Cu catalyst, however, the metal particles were easily aggregated after the reduction and resulted in larger particle sizes (Figure S1). The alloy phase of the CuNi particles as indicated in the XRD analysis was further confirmed by HRTEM as shown in Figure S2. The lattice fringe of the selected domain was measured to be 0.205 nm, which was just right between the pure Ni(111) and Cu(111) planes (0.202 and 0.210 nm, respectively). Apart from that, the metallic Cu phase was also found in another HRTEM picture, showing a lattice fringe of ~0.210 nm. These

results corresponded well to the XRD results that both metallic Cu and CuNi alloy phases were existed in the as-prepared catalysts.

The textural properties of the Cu–Ni catalysts are summarized in Table 1. Al$_2$O$_3$ had a moderate BET surface area of 222.4 m^2/g, and the total pore volume was 0.72 cm^3/g with an average pore size of 12.9 nm. After it was immobilized with Cu and Ni metals, the BET surface area decreased slightly (Table 1, entries 2–4). Noteworthy, the pore volume/size continually decreased as the Ni loading increased, which might be resulted from the block of the pores as more metals were incorporated into the Al$_2$O$_3$ structure.

Initial Catalyst Screening. The screening of the catalysts for the conversion of EL to GVL was carried out by using 2-BuOH as the hydrogen donor. It was a commonly used agent in the CTH reaction.[46] When 10Cu-1Ni/Al$_2$O$_3$ was subjected to the model reaction at 150 °C, the reaction gave a 90% yield of GVL at 98% conversion of EL in 12 h (Table 2, entry 1). As the weight percentage of Ni increased in the Cu–Ni catalyst, higher GVL yields were obtained, 92% and 97% for 10Cu-3Ni/Al$_2$O$_3$ and 10Cu-5Ni/Al$_2$O$_3$, respectively (Table 2, entries 2 and 3). The increase of Ni loading may bring two advantages: (1) more hydrogenating sites from Ni particles would formed and enhanced the hydrogenation ability of the catalysts; (2) more Ni would interacted with Cu to form alloys or geometry metal cluster size, which could inhibit the metal sintering processes and result in metal particles with smaller sizes (particles with smaller size are postulated to have higher reactivity).[57] However, further increasing the Cu weight percentage from 10 to 15 wt % led to a lower GVL yield of 84% at 90% EL conversion (Table 2, entry 4). It was probably caused by excessive loading of Cu that led to larger particle sizes and thereby decreased the catalyst's reactivity. Therefore, a 10:5 weight ratio of Cu–Ni was the optimal ratio for the catalyst supported on Al$_2$O$_3$. Other Cu–Ni catalysts supported on a variety of metal oxides were also investigated in the CTH reaction. Cu–Ni catalysts supported on TiO$_2$ or SiO$_2$ provided much lower yields of GVL (Table 2, entries 5 and 6). And those catalysts supported on SiO$_2$–Al$_2$O$_3$ and ZrO$_2$ provided comparable GVL yields to that from 10Cu-5Ni/Al$_2$O$_3$ catalyst (Table 2, entries 7 and 8). The acid–base nature of these supports may be responsible for different performances of these catalysts. Previous research revealed that the supports with more acid–base sites were favored for the CTH reaction,[47] which could assist the dehydrogenation of the alcohols by forming alkoxide on the catalyst's surface and then facilitate the migration of H to unsaturation over metal sites. Zirconium oxide and aluminum oxide are such type of supports that are rich in acid–base sites in the structure, therefore exhibiting better performances in the CTH reactions. These results further highlighted the important roles of the supports on the reactivity of the catalyst

To explore further the catalytic role of Cu and Ni in the CTH reaction, monometallic Cu and Ni catalysts supported on Al$_2$O$_3$ were also prepared and used in the CTH reaction to compare their reactivities. For 10Cu/Al$_2$O$_3$ catalyst, 86% yield of GVL was obtained at 92% conversion of EL (Table 2, entry 9). However, for 5Ni/Al$_2$O$_3$, it only provided 26% yield of GVL with 30% conversion of EL (Table 2, entry 10). Previous work reported that Ni possessed high reactivity for the CTH reaction when at its zerovalent state.[50] However, the current monometallic Ni catalyst was reluctant to be reduced when it was immobilized on Al$_2$O$_3$ support due to its strong interaction
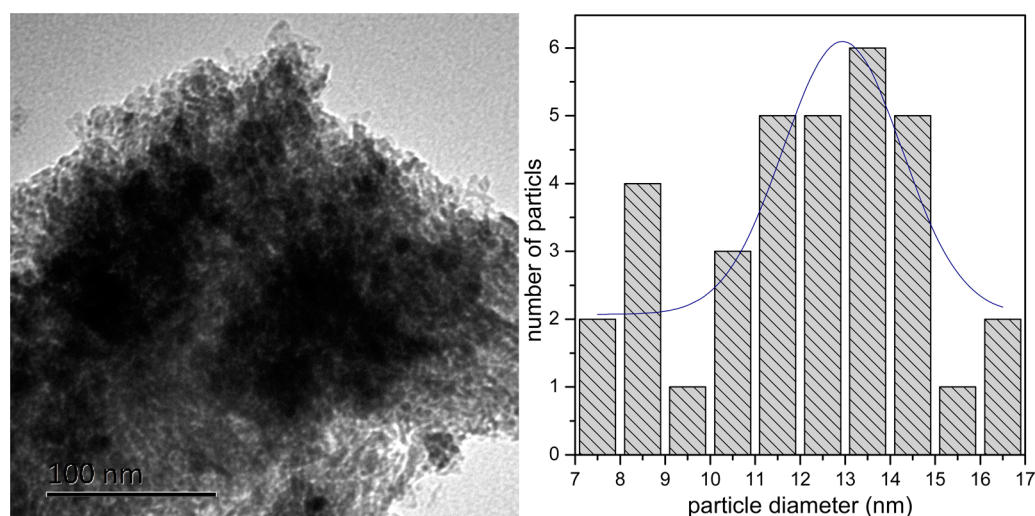
Figure 8. TEM analysis of the spent 10Cu-5Ni/Al$_2$O$_3$ catalyst.
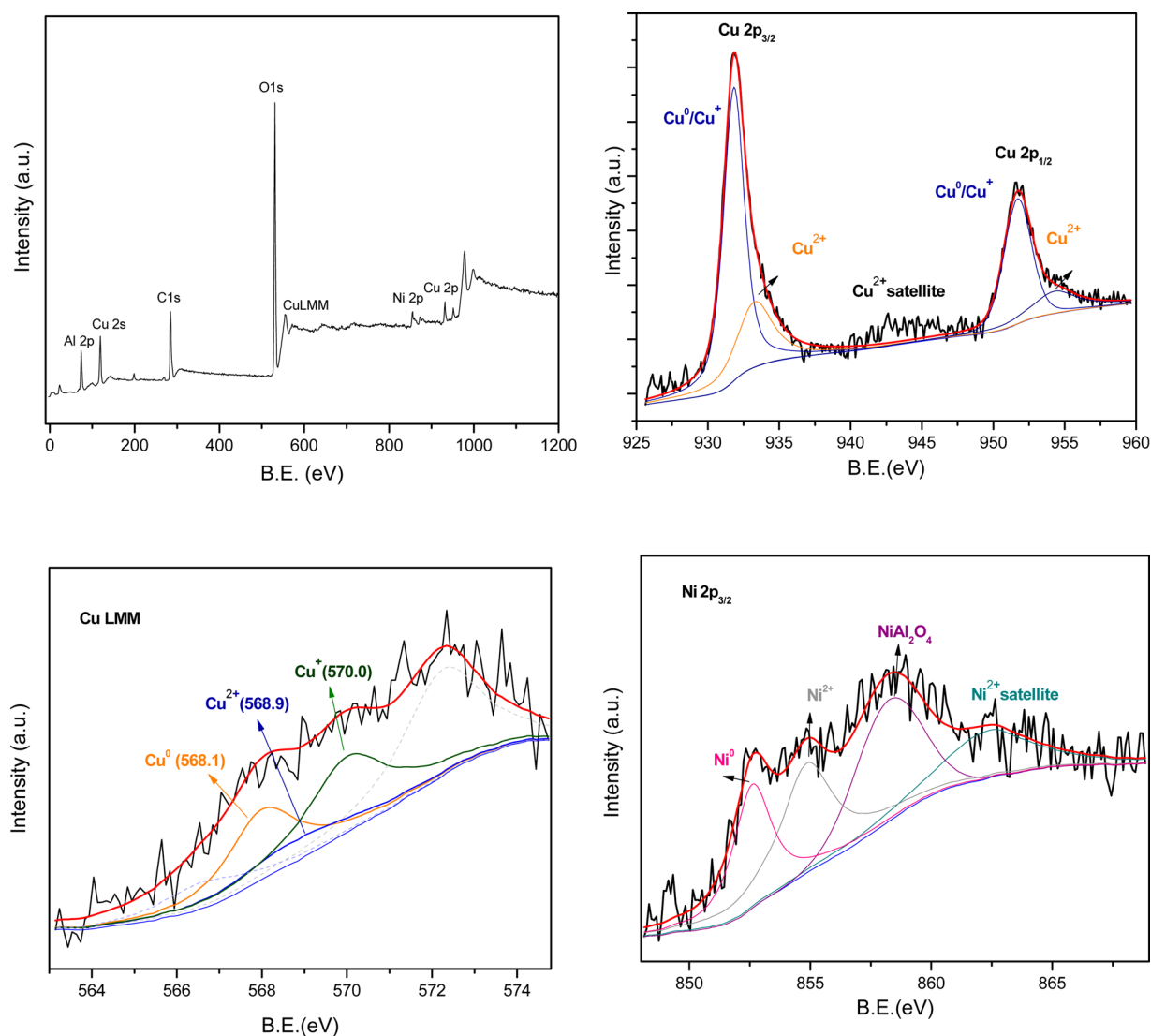
Figure 9. XPS analysis of the spent 10Cu-5Ni/Al$_2$O$_3$ catalyst: survey, Cu 2p, Cu LMM and Ni 2p.

with the support (Figure S3). The presence of Cu could lower the reduction temperature of Ni species in the bimetallic Cu−Ni catalyst and provided more reduced Ni sites.[62] Physical

mixing of the two catalysts and subjecting them to the reaction led to a lower GVL yield (70%) than those from either of the single monometallic catalysts (Table 2, entry 11). This result

implied that the mixed phases the Cu and Ni metals or alloys were key to the high activity of the bimetallic Cu−Ni catalyst. To exam whether the system was tolerant to moisture and air, 5 wt % of water was added to the reaction system, and a slightly decreased GVL yield of 87% was obtained (Table 2, entry 12). Even when the reaction was performed in the atmosphere condition, it could still provide 86% yield of GVL at 91% conversion of EL (Table 2, entry 13). A blank experiment was also carried out with Al_2O_3 as catalyst; the reaction only provided 18% yield of GVL under the standard reaction condition, further conforming the significance of metal sites in the catalysis. These results further demonstrated that the 10Cu-3Ni/Al_2O_3 catalyst had a good tolerance to the environmental condition in the conversion of EL to GVL.

Effect of Reaction Temperature and Time. The reaction temperature has a profound effect on the reaction rate. Thus, the CTH of EL was carried out at different reaction temperatures, ranging from 120 to 160 °C (Figure 4a). When the reaction proceeded at a milder condition (120 °C), 79% yield of GVL was achieved. With the increase of the reaction temperature, the EL conversion and GVL yield continuously increased until a maximum GVL yield of 97% was obtained at 150 °C. This was possibly attributed to the increase of the reaction rate at higher reaction temperature. Further increasing the reaction temperature to 160 °C led to a slight decrease of GVL yield. It was likely that the product might undergo some side reactions and generate unknown products at higher reaction temperature. Accordingly, the reaction temperature was kept at 150 °C for the following reaction. Meanwhile, the reaction was also traced to investigate the influence of the reaction time on the CTH reaction (Figure 4b). The reaction reached 60% yield of GVL in 2 h and the product yield gradually increased as the reaction proceeded. The maximum yield occurred at 12 h. Further prolonging the reaction time resulted in a slight decrease of the product yield. Based on the above experiments, the optimal reaction temperature of 150 °C and reaction time of 12 h were sufficient for the CTH reaction to achieve high produce yield.

Effect of Catalyst Loading. The influence of catalyst loading on the efficiency of the CTH reaction was also investigated by varying the 10Cu-5Ni/Al_2O_3 loading from 60 to 120 mg while other reaction conditions remained unchanged. As shown in Table 3, only 74% EL conversion was obtained when the catalyst loading was 60 mg, yielding 71% yield of GVL (Table 3, entry 1). With the increase of the catalyst loading, the reaction showed higher GVL yields until 97% yield of GVL was provided at 100 mg of catalyst loading (Table 3, entries 2 and 3). A further increase of the catalyst loading to 120 mg led to a slight decrease in the GVL yield, possibly attributed to some side reactions over excess metallic catalyst sites. Noteworthy, the reaction can also proceed well at a lower loading of catalyst by extending the reaction time. For example, the CTH of EL with 60 mg of catalyst provided 96% yield of GVL when prolonging the reaction time to 24 h. This result suggested that the Cu−Ni catalysts exhibited high reactivity toward the CTH of EL to GVL.

Substrate and Solvent Scope. With the optimized reaction condition in hand, we next turn to the substrate and solvent scope of the CTH reaction, as shown in Table 4. The CTH reaction with primary alcohols as the H-donors provided low GVL product yields, which was consistent with many previously reported works. The primary alcohols were poor H-donors in the CTH reaction due to the difficult β-hydride

elimination after it formed alkoxy species on the surface of the catalyst (Table 4, entries 1 and 2).[49] For secondary alcohols, the reaction with i-PrOH provides 75% yield of GVL whereas that with 3-pentanol afforded 97% yield of GVL (Table 4, entries 3 and 4). Further prolonging the reaction time to 24 h provided a higher GVL yield of 87%. Besides, cyclohexanol (CyOH) was also an effective H-donor for the CTH of EL to GVL and a moderate yield of 81% was obtained with 89% EL conversion (Table 4, entry 5). 2-Butanol was selected as the H-donor for the CTH of EL to produce GVL in our system in terms of its reactivity as well as the practical point of view. These results further highlighted the traditional transfer hydrogenation reaction mechanism of our system: secondary alcohol was first absorbed on the surface of the catalyst and formed alkoxide species by dissociation its O—H bond. The alkoxide species subsequently underwent β-hydride elimination to form metal hydride species and release the side product (e.g., acetone if using 2-PrOH). The unsaturated C=O bond of EL was then hydrogenated by the active metal hydride species to yield ethyl 4-hydroxypentanoate, which finally underwent intramolecular cyclization and formed GVL.

Other levulinate esters were also applied to the CTH reaction for the production of GVL. Methyl- and butyl levulinate were successfully converted to GVL at 94% and 95% yield, respectively (Table 4, entries 6 and 7). Noteworthy, when levulinic acid was subjected to the CTH reaction, only a small amount of GVL was obtained (<10%) and the reaction solution turned blue (Table 4, entry 8). This might be resulted from the acidic nature of LA that could react with the weak basic support Al_2O_3, leading to the collapse of the support and the leach of metal sites into the reaction solution. Overall, the 10Cu-5Ni/Al_2O_3 catalyst showed excellent performance in the CTH of various levulinate esters to GVL with different secondary alcohols.

Stability of Catalyst. To investigate the stability of the Cu−Ni catalyst, the monometallic Cu catalyst was also selected as the benchmark catalyst for the CTH reaction under the optimized reaction condition, as shown in Figure 5. For the freshly prepared catalysts, 10Cu/Al_2O_3 provided 86% yield of GVL whereas 10Cu-5Ni/Al_2O_3 afforded 97% yield of GVL. When both of the catalysts were exposed in air for 1 week and then subjected to the model reaction, 10Cu/Al_2O_3 provided only 3% yield of GVL, suggesting the severe deactivation the catalyst through gradual oxidation in the air. In contrast, 10Cu-5Ni/Al_2O_3 provided 87% yield of GVL, only a slight decrease compared to the fresh ones. 10Cu-5Ni/Al_2O_3 was very stable and resistant against the oxidation in the air. As reported in many previous works,[57,63] the use of a bimetallic catalyst had several advantages over their monometallic counterparts including stabilizing effects and ligand effect. The addition of a metal promoter could inhibit the sintering of metal particles or suppress the formation of carbonaceous deposits on the surface of catalyst. Besides, the metal could also act as a ligand that alters the electron properties of the actives sites, resulting in a more robust catalyst. Therefore, a bimetallic one may exhibit good stability toward air oxidation. In addition, when these two catalysts were recycled from the reaction mixture and subjected to the next run, they exhibited better performances, yielding 10% and 96% yield of GVL, respectively, even higher than those of their first runs. This catalyst underwent an *in situ* reduction during the first catalytic run and more oxidized metal particles were further reduced and became more reactive (discussed later). Based on these results, it can be concluded

that the 10Cu-5Ni/Al$_2$O$_3$ was a very stable catalyst in the air and maintain a high reactivity in the CTH reaction. Moreover, the CTH reaction system was a reductive system that could prevent the catalyst from being easily oxidized.

Catalyst Recycling and Characterization. To investigate further the recyclability of the 10Cu-5Ni/Al$_2$O$_3$ catalyst, catalyst recycle tests for the CTH of EL to GVL were performed under the optimized reaction condition. After each run, the catalyst was separated by centrifuge, washed with the fresh solvent and then directly subjected to the next run. The results are presented in Figure 6. The catalyst was used for 10 catalytic runs with only a slight decrease in the EL conversion and the GVL yield, yielding 93% yield of GVL in the tenth run.

To figure out the change of the catalyst during the reaction, the spent catalyst was collected and characterized. Figure 7 shows the XRD analysis of the fresh and spent catalysts. The two patterns showed similar diffraction peaks, which indicated that the active metal sites on the surface of the catalyst were almost unchanged during the CTH reaction. TEM characterization of the spent catalyst showed that no obvious change in the surface morphology of the catalyst, and the metal particles still well dispersed after the reaction (Figure 8). However, the average sizes of the metal particles became a little larger (12−13 nm). This might be caused by the aggregation of the metal sites in thermal solutions, which might be unavoidable for most supported monometallic catalyst under such reaction condition. However, the reactivity of the catalyst still remained at a high level in spite of the larger particle sizes. This result further confirmed that 10Cu-5Ni/Al$_2$O$_3$ catalyst had an excellent stability under the CTH reaction condition.

XPS analysis of the spent catalyst showed major changes of the oxidation state of the metal species (Figure 9). For Cu 2p$_{3/2}$, the peak located at 932.3 eV, corresponded to Cu^0/Cu$^+$ crystallite species, became stronger compared to the fresh catalyst whereas the peak at 934.2 eV (Cu^{2+}) became weaker, as well as its satellite peak round 944 eV. This result apparently showed that more Cu^{2+} crystallite species were reduced to Cu^0/Cu$^+$ species during the CTH reaction. The Cu LMM spectrum of the spent catalyst further confirmed this result in which the Cu^{2+} peak became weaker compared to the fresh catalyst and the area ratio of Cu^0, Cu^{2+} and Cu$^+$ was 1:0.46:1.08. Comparing with the fresh catalyst, more of Cu^{2+} and Cu$^+$ species were reduced during the reaction. Moreover, high-valent Ni^{2+} crystallite species were also partially reduced during the reaction and more Ni^0 was formed. These reduced metal sites may provide more hydrogenating sites and increased the reactivity of the recycled catalyst in the CTH reaction, which was in line with the excellent activity of Cu−Ni catalyst in the recycling experiments. This was also an appealing advantage of the CTH reaction in that it can protect the metallic catalyst from losing reactivity by oxidation.

CONCLUSION

In this study, we reported a robust and efficient Cu−Ni bimetallic catalyst for the transfer hydrogenation of biomass derived levulinate esters to γ-valerolactone. An optimal 10:5 weight ratio of Cu to Ni was found to have the highest catalytic activity in the CTH reaction, providing the highest GVL yield of 97% by using 2-butanol as the H-donor at 150 °C for 12 h. Characterization of the fresh and spent catalyst showed that the synergy between Cu and Ni particles were responsible for the high stability and reactivity of the bimetallic catalyst, which enabled a 10 times of catalyst recycling. Besides, the CTH

system also provided an effective *in situ* reduction environment for keeping the Cu−Ni catalyst in high reactivity. This new robust and efficient catalyst may also find other important applications in the CTH of other biomass derived raw materials to produce more value-added compounds.

ASSOCIATED CONTENT

Ⓢ Supporting Information

The Supporting Information is available free of charge on the ACS Publications website at DOI: 10.1021/acssusche-meng.6b01677.

Additional details on the characterization of the catalysts and reaction optimization results (PDF)

AUTHOR INFORMATION

Corresponding Authors
*Yao-Bing Huang (Email: hyb123@mail.ustc.edu.cn), Tel: (86) 25-85428173.
*Hui Pan (Email: hpan@njfu.edu.cn).

ORCID Ⓒ
Hui Pan: 0000-0001-5074-8314
Yao-Bing Huang: 0000-0002-3783-862X

Author Contributions
‡These authors equally contributed to the work. All authors have given approval to the final version of the paper.

Notes
The authors declare no competing financial interest.

ACKNOWLEDGMENTS

REFERENCES

(1) Corma, A.; Iborra, S.; Velty, A. Chemical routes for the transformation of biomass into chemicals. *Chem. Rev.* **2007**, *107* (6), 2411−2502.
(2) Besson, M.; Gallezot, P.; Pinel, C. Conversion of Biomass into Chemicals over Metal Catalysts. *Chem. Rev.* **2014**, *114* (3), 1827−1870.
(3) Serrano-Ruiz, J. C.; Dumesic, J. A. Catalytic routes for the conversion of biomass into liquid hydrocarbon transportation fuels. *Energy Environ. Sci.* **2011**, *4* (1), 83−99.
(4) Huber, G. W.; Chheda, J. N.; Barrett, C. J.; Dumesic, J. A. Production of liquid alkanes by aqueous-phase processing of biomass-derived carbohydrates. *Science* **2005**, *308* (5727), 1446−1450.
(5) Li, G.; Li, N.; Yang, J.; Li, L.; Wang, A.; Wang, X.; Cong, Y.; Zhang, T. Synthesis of renewable diesel range alkanes by hydro-deoxygenation of furans over Ni/Hβ under mild conditions. *Green Chem.* **2014**, *16* (2), 594−599.
(6) Zhao, C.; Brück, T.; Lercher, J. A. Catalytic deoxygenation of microalgae oil to green hydrocarbons. *Green Chem.* **2013**, *15* (7), 1720−1739.
(7) Wang, A.; Zhang, T. One-Pot Conversion of Cellulose to Ethylene Glycol with Multifunctional Tungsten-Based Catalysts. *Acc. Acc. Chem. Res.* **2013**, *46* (7), 1377−1386.
(8) Hausoul, P. C.; Negahdar, L.; Schute, K.; Palkovits, R. Unravelling the Ru-Catalyzed Hydrogenolysis of Biomass-Based

Polyols under Neutral and Acidic Conditions. *ChemSusChem* **2015**, *8* (19), 3323−3330.

(9) Chen, K.; Mori, K.; Watanabe, H.; Nakagawa, Y.; Tomishige, K. J. C−O bond hydrogenolysis of cyclic ethers with OH groups over rhenium-modified supported iridium catalysts. *J. Catal.* **2012**, *294*, 171−183.

(10) Liu, X.; Wang, X.; Yao, S.; Jiang, Y.; Guan, J.; Mu, X. Recent advances in the production of polyols from lignocellulosic biomass and biomass-derived compounds. *RSC Adv.* **2014**, *4* (90), 49501−49520.

(11) Fabičovicová, K.; Lucas, M.; Claus, P. From microcrystalline cellulose to hard-and softwood-based feedstocks: their hydrogenolysis to polyols over a highly efficient ruthenium−tungsten catalyst. *Green Chem.* **2015**, *17* (5), 3075−3083.

(12) de Souza, R. O. M. A.; Miranda, L. S. M.; Luque, R. Bio (chemo) technological strategies for biomass conversion into bioethanol and key carboxylic acids. *Green Chem.* **2014**, *16* (5), 2386−2405.

(13) Dutta, S.; Wu, L.; Mascal, M. Efficient metal-free production of succinic acid by oxidation of biomass-derived levulinic acid with hydrogen peroxide. *Green Chem.* **2015**, *17* (4), 2335−2338.

(14) Mei, N.; Liu, B.; Zheng, J.; Lv, K.; Tang, D.; Zhang, Z. A novel magnetic palladium catalyst for the mild aerobic oxidation of 5-hydroxymethylfurfural into 2, 5-furandicarboxylic acid in water. *Catal. Sci. Technol.* **2015**, *5* (6), 3194−3202.

(15) Yi, G.; Teong, S. P.; Zhang, Y. Base-free conversion of 5-hydroxymethylfurfural to 2, 5-furandicarboxylic acid over a Ru/C catalyst. *Green Chem.* **2016**, *18* (4), 979−983.

(16) Ding, D.; Xi, J.; Wang, J.; Liu, X. G.; Wang, Y.; Lu, G. Production of methyl levulinate from cellulose: selectivity and mechanism study. *Green Chem.* **2015**, *17* (7), 4037−4044.

(17) Weingarten, R.; Conner, W. C.; Huber, G. W. Production of levulinic acid from cellulose by hydrothermal decomposition combined with aqueous phase dehydration with a solid acid catalyst. *Energy Environ. Sci.* **2012**, *5* (6), 7559−7574.

(18) Démolis, A.; Essayem, N.; Rataboul, F. Synthesis and Applications of Alkyl Levulinates. *ACS Sustainable Chem. Eng.* **2014**, *2* (6), 1338−1352.

(19) Mariscal, R.; Maireles-Torres, P.; Ojeda, M.; Sádaba, I.; López Granados, M. Furfural: a renewable and versatile platform molecule for the synthesis of chemicals and fuels. *Energy Environ. Sci.* **2016**, *9* (4), 1144−1189.

(20) Lange, J.; van der Heide, E.; van Buijtenen, J.; Price, R. Furfural-a promising platform for lignocellulosic biofuels. *ChemSusChem* **2012**, *5* (1), 150−166.

(21) Horvath, I. T.; Mehdi, H.; Fabos, V.; Boda, L.; Mika, L. T. *γ*-Valerolactone-a sustainable liquid for energy and carbon-based chemicals. *Green Chem.* **2008**, *10* (2), 238−242.

(22) Liguori, F.; Moreno-Marrodan, C.; Barbaro, P. Environmentally Friendly Synthesis of *γ*-Valerolactone by Direct Catalytic Conversion of Renewable Sources. *ACS Catal.* **2015**, *5* (3), 1882−1894.

(23) Lange, J.; Price, R.; Ayoub, P. M.; Louis, J.; Petrus, L.; Clarke, L.; Gosselink, H. Valeric biofuels: a platform of cellulosic transportation fuels. Angew. *Angew. Chem., Int. Ed.* **2010**, *49* (26), 4479−4483.

(24) Sun, P.; Gao, G.; Zhao, Z.; Xia, C.; Li, F. Acidity-regulation for enhancing the stability of Ni/HZSM-5 catalyst for valeric biofuel production. *Appl. Catal., B* **2016**, *189*, 19−25.

(25) Li, M.; Li, G.; Li, N.; Wang, A.; Dong, W.; Wang, X.; Cong, Y. Aqueous phase hydrogenation of levulinic acid to 1, 4-pentanediol. *Chem. Commun.* **2014**, *50* (12), 1414−1416.

(26) Mizugaki, T.; Nagatsu, Y.; Togo, K.; Maeno, Z.; Mitsudome, T.; Jitsukawa, K.; Kaneda, K. Selective hydrogenation of levulinic acid to 1, 4-pentanediol in water using a hydroxyapatite-supported Pt-Mo bimetallic catalyst. *Green Chem.* **2015**, *17* (12), 5136−5139.

(27) Wright, W. R. H.; Palkovits, R. Development of Heterogeneous Catalysts for the Conversion of Levulinic Acid to *γ*-Valerolactone. *ChemSusChem* **2012**, *5* (9), 1657−1667.

(28) Manzer, L. E. Catalytic synthesis of *α*-methylene-*γ*-valerolactone: a biomass-derived acrylic monomer. *Appl. Catal., A* **2004**, *272* (1−2), 249−256.

(29) Upare, P. P.; Lee, J.-M.; Hwang, D. W.; Halligudi, S. B.; Hwang, Y. K.; Chang, J.-S. J.Selective hydrogenation of levulinic acid to *γ*-valerolactone over carbon-supported noble metal catalysts. *J. Ind. Eng. Chem.* **2011**, *17* (2), 287−292.

(30) Yan, Z.; Lin, L.; Liu, S. Synthesis of *γ*-valerolactone by hydrogenation of biomass-derived levulinic acid over Ru/C catalyst. *Energy Fuels* **2009**, *23* (8), 3853−3858.

(31) Chalid, M.; Broekhuis, A. A.; Heeres, H. J. Experimental and kinetic modeling studies on the biphasic hydrogenation of levulinic acid to *γ*-valerolactone using a homogeneous water-soluble Ru-(TPPTS) catalyst. *J. Mol. Catal. A: Chem.* **2011**, *341* (1−2), 14−21.

(32) Galletti, A. M. R.; Antonetti, C.; De Luise, V.; Martinelli, M. A sustainable process for the production of *γ*-valerolactone by hydrogenation of biomass-derived levulinic acid. *Green Chem.* **2012**, *14* (3), 688−694.

(33) Al-Shaal, M. G.; Wright, W. R. H.; Palkovits, R. Exploring the ruthenium catalysed synthesis of *γ*-valerolactone in alcohols and utilisation of mild solvent-free reaction conditions. *Green Chem.* **2012**, *14* (5), 1260−1263.

(34) Schuette, H. A.; Thomas, R. W. Normal valerolactone. III. Its preparation by the catalytic reduction of levulinic acid with hydrogen in the presence of platinum oxide. *J. Am. Chem. Soc.* **1930**, *52* (7), 3010−3012.

(35) Zhou, H.; Song, J.; Fan, H.; Zhang, B.; Yang, Y.; Hu, J.; Zhu, Q.; Han, B. Cobalt catalysts: very efficient for hydrogenation of biomass-derived ethyl levulinate to gamma-valerolactone under mild conditions. *Green Chem.* **2014**, *16* (8), 3870−3875.

(36) Upare, P. P.; Lee, J. M.; Hwang, Y. K.; Hwang, D. W.; Lee, J. H.; Halligudi, S. B.; Hwang, J. S.; Chang, J. S. Direct Hydrocyclization of Biomass-Derived Levulinic Acid to 2-Methyltetrahydrofuran over Nanocomposite Copper/Silica Catalysts. *ChemSusChem* **2011**, *4* (2), 1749−1752.

(37) Shimizu, K.; Kanno, S.; Kon, K. Hydrogenation of levulinic acid to *γ*-valerolactone by Ni and MoO_x co-loaded carbon catalysts. *Green Chem.* **2014**, *16* (8), 3899.

(38) Kumar, V. V.; Naresh, G.; Sudhakar, M.; Anjaneyulu, C.; Bhargava, S. K.; Tardio, J.; Reddy, V. K.; Padmasri, A. H.; Venugopal, A. An investigation on the influence of support type for Ni catalysed vapour phase hydrogenation of aqueous levulinic acid to *γ*-valerolactone. *RSC Adv.* **2016**, *6* (12), 9872−9879.

(39) Mohan, V.; Venkateshwarlu, V.; Pramod, C. V.; Raju, B. D.; Rao, K. S. R. Vapour phase hydrocyclisation of levulinic acid to *γ*-valerolactone over supported Ni catalysts. *Catal. Sci. Technol.* **2014**, *4* (5), 1253−1259.

(40) Zhang, J.; Chen, J.; Guo, Y.; Chen, L. Effective Upgrade of Levulinic Acid into *γ*-Valerolactone over an Inexpensive and Magnetic Catalyst Derived from Hydrotalcite Precursor. *ACS Sustainable Chem. Eng.* **2015**, *3* (8), 1708−1714.

(41) Deng, L.; Li, J.; Lai, D. M.; Fu, Y.; Guo, Q. X. Catalytic conversion of biomass-derived carbohydrates into *γ*-valerolactone without using an external H_2 supply. *Angew. Chem., Int. Ed.* **2009**, *48* (35), 6529−6532.

(42) Saravanamurugan, S.; Van Buu, O. N.; Riisager, A. Conversion of Mono- and Disaccharides to Ethyl Levulinate and Ethyl Pyranoside with Sulfonic Acid-Functionalized Ionic Liquids. *ChemSusChem* **2011**, *4* (6), 723−726.

(43) Hu, X.; Li, C. Z. Levulinic esters from the acid-catalysed reactions of sugars and alcohols as part of a bio-refinery. *Green Chem.* **2011**, *13* (7), 1676−1679.

(44) Shimizu, K. Heterogeneous catalysis for the direct synthesis of chemicals by borrowing hydrogen methodology. *Catal. Sci. Technol.* **2015**, *5* (3), 1412−1427.

(45) Gilkey, M. J.; Xu, B. Heterogeneous Catalytic Transfer Hydrogenation as an Effective Pathway in Biomass Upgrading. *ACS Catal.* **2016**, *6* (3), 1420−1436.

(46) Chia, M.; Dumesic, J. A. Liquid-phase catalytic transfer hydrogenation and cyclization of levulinic acid and its esters to γ-valerolactone over metal oxide catalysts. *Chem. Commun.* **2011**, *47* (44), 12233−12235.

(47) Tang, X.; Hu, L.; Sun, Y.; Zhao, G.; Hao, W.; Lin, L. Conversion of biomass-derived ethyl levulinate into γ-valerolactone via hydrogen transfer from supercritical ethanol over a ZrO_2 catalyst. *RSC Adv.* **2013**, *3* (26), 10277−10284.

(48) Song, J.; Wu, L.; Zhou, B.; Zhou, H.; Fan, H.; Yang, Y.; Meng, Q.; Han, B. A new porous Zr-containing catalyst with a phenate group: an efficient catalyst for the catalytic transfer hydrogenation of ethyl levulinate to γ-valerolactone. *Green Chem.* **2015**, *17* (3), 1626−1632.

(49) Kuwahara, Y.; Kaburagi, W.; Fujitani, T. Catalytic transfer hydrogenation of levulinate esters to γ-valerolactone over supported ruthenium hydroxide catalysts. *RSC Adv.* **2014**, *4* (86), 45848−45855.

(50) Yang, Z.; Huang, Y.; Guo, Q.; Fu, Y. RANEY® Ni catalyzed transfer hydrogenation of levulinate esters to γ-valerolactone at room temperature. *Chem. Commun.* **2013**, *49* (46), 5328−5330.

(51) Li, H.; Fang, Z.; Yang, S. Direct Catalytic Transformation of Biomass Derivatives into Biofuel Component γ-Valerolactone with Magnetic Nickel-Zirconium Nanoparticles. *ChemPlusChem* **2016**, *81* (1), 135−142.

(52) Yang, Y.; Xu, X.; Zou, W.; Yue, H.; Tian, G.; Feng, S. Transfer hydrogenation of methyl levulinate into gamma-valerolactone, 1, 4-pentanediol, and 1-pentanol over Cu−ZrO_2 catalyst under solvothermal conditions. *Catal. Commun.* **2016**, *76*, 50−53.

(53) Swarna Jaya, V.; Sudhakar, M.; Naveen Kumar, S.; Venugopal, A. Selective hydrogenation of levulinic acid to γ-valerolactone over a Ru/Mg−LaO catalyst. *RSC Adv.* **2015**, *5* (12), 9044−9049.

(54) Li, Z.; Tang, X.; Jiang, Y.; Wang, Y.; Zuo, M.; Chen, W.; Zeng, X.; Sun, Y.; Lin, L. Atom-economical synthesis of γ-valerolactone with self-supplied hydrogen from methanol. *Chem. Commun.* **2015**, *51* (91), 16320−16323.

(55) Gowda, R. R.; Chen, E. Y.-X. Recyclable Earth-Abundant Metal Nanoparticle Catalysts for Selective Transfer Hydrogenation of Levulinic Acid to Produce γ-Valerolactone. *ChemSusChem* **2016**, *9* (2), 181−185.

(56) Zaccheria, F.; Ravasio, N.; Psaro, R.; Fusi, A. Synthetic scope of alcohol transfer dehydrogenation catalyzed by Cu/Al_2O_3: A new metallic catalyst with unusual selectivity. *Chem. - Eur. J.* **2006**, *12* (24), 6426−6431.

(57) Martin, D. A.; Wettstein, S. G.; Dumesic, J. A. Bimetallic catalysts for upgrading of biomass to fuels and chemicals. *Chem. Soc. Rev.* **2012**, *41* (24), 8075−8098.

(58) Chang, X.; Liu, A. F.; Cai, B.; Luo, J. Y.; Pan, H.; Huang, Y. B. Catalytic Transfer Hydrogenation of Furfural to 2-Methylfuran and 2-Methyltetrahydrofuran over Bimetallic Copper−Palladium Catalysts. *ChemSusChem* **2016**, *9*, 3330.

(59) Kannapu, H. P. R.; Mullen, C. A.; Elkasabi, Y.; Boateng, A. A. Catalytic transfer hydrogenation for stabilization of bio-oil oxygenates: Reduction of p-cresol and furfural over bimetallic Ni−Cu catalysts using isopropanol. *Fuel Process. Technol.* **2015**, *137*, 220−228.

(60) Wu, Q.; Eriksen, W. L.; Duchstein, L. D. L.; Christensen, J. M.; Damsgaard, C. D.; Wagner, J. B.; Temel, B.; Grunwaldt, J. D.; Jensen, A. D. Influence of preparation method on supported Cu−Ni alloys and their catalytic properties in high pressure CO hydrogenation. *Catal. Sci. Technol.* **2014**, *4* (2), 378−386.

(61) Jha, A.; Jeong, D.; Shim, J.; Jang, W.; Lee, Y.; Rode, C. V.; Roh, H. Hydrogen production by the water-gas shift reaction using CuNi/Fe_2O_3 catalyst. *Catal. Sci. Technol.* **2015**, *5* (5), 2752−2760.

(62) Gandarias, I.; Arias, P. L.; Requies, J.; El Doukkali, M.; Guemez, M. B. Liquid-phase glycerol hydrogenolysis to 1, 2-propanediol under nitrogen pressure using 2-propanol as hydrogen source. *J. Catal.* **2011**, *282* (1), 237−247.

(63) Fang, H.; Wen, M.; Chen, H.; Wu, Q.; Li, W. Graphene stabilized ultra-small CuNi nanocomposite with high activity and recyclability toward catalysing the reduction of aromatic nitro-compounds. *Nanoscale* **2016**, *8* (1), 536−542.